Contents lists available at ScienceDirect

BBA - Biomembranes

journal homepage: www.elsevier.com

Studies on interaction of green silver nanoparticles with whole bacteria by surface characterization techniques

Anike P.V. Ferreyra Maillard [a], Sónia Gonçalves [b], Nuno C. Santos [b], Beatriz A. López de Mishima [a], Pablo R. Dalmasso [c, *], Axel Hollmann [b, d, e, **]

[a] INBIONATEC, CONICET, Universidad Nacional de Santiago del Estero, RN 9, Km 1125, 4206 Santiago del Estero, Argentina
[b] Instituto de Medicina Molecular, Faculdade de Medicina, Universidade de Lisboa, Lisbon, Portugal
[c] CIQA, CONICET, Departamento de Ingeniería Química, Facultad Regional Córdoba, Universidad Tecnológica Nacional, Maestro López esq. Cruz Roja Argentina, 5016 Córdoba, Argentina
[d] Laboratorio de Compuestos Bioactivos, Centro de Investigaciones en Biofísica Aplicada y Alimentos (CIBAAL), CONICET, Universidad Nacional de Santiago del Estero, RN 9, Km 1125, 4206 Santiago del Estero, Argentina
[e] Laboratorio de Microbiología Molecular, Instituto de Microbiología Básica y Aplicada, Universidad Nacional de Quilmes, Roque Saenz Peña 352, B1876BXD Bernal, Argentina

ARTICLE INFO

Keywords:
Silver nanoparticles
Green synthesis
Lipid interaction
Antimicrobial activity
Atomic force microscopy

ABSTRACT

The use of silver nanoparticles (AgNPs) with their novel and distinct physical, chemical, and biological properties, has proven to be an alternative for the development of new antibacterial agents. In particular, the possibility to generate AgNPs coated with novel capping agents, such as phytomolecules obtained *via* a green synthesis (G-AgNPs), is attracting great attention in scientific research.

Recently, we showed that membrane interactions seem to be involved in the antibacterial activity of AgNPs obtained *via* a green chemical synthesis using the aqueous leaf extract of chicory (*Cichorium intybus* L.). Furthermore, we observed that these G-AgNPs exhibited higher antibacterial activity than those obtained by chemical synthesis.

In order to achieve the green AgNPs mode of action as well as their cellular target, we aimed to study the antibacterial activity of this novel green AgNPs against Gram-negative (*Escherichia coli*) and Gram-positive (*Staphylococcus aureus*) bacteria. The effect of the G-AgNPs on the bacterial surface was first evaluated by zeta potential measurements and correlated with direct plate count agar method. Afterwards, atomic force microscopy was applied to directly unravel the effects of these G-AgNPs on bacterial envelopes.

Overall, the data obtained in this study seems correlated with a multi-step mechanism by which electrostatic interactions is the first step prior to membrane disruption, resulting in antibacterial activity.

1. Introduction

Nowadays, resistance to the main antibiotics currently used in the clinic has been reaching a critical level, which has resulted in a significant threat to public health [1–3]. One of the recent efforts in addressing this current scenario lies in reexploring the biological properties of already known antimicrobial materials by manipulating their size to the nanoscale to which microbial pathogens may not be able to develop resistance [4]. In this context, the silver-containing nanosystems, notably silver nanoparticles (AgNPs), polymer/metal nanocomposites, and magnetic nanostructures, have attracted great attention due to they are one of the most promising nanostructures right now for the development of new antibacterial agents, with potential applications in both the pharmaceutical and biomedical fields as growth inhibitors, killing agents, or antimicrobial carriers [5–13]. Thus, AgNPs impregnated in biomedical materials, such as collagen, have shown biocompatibility and enhanced antibacterial activity highlighting their potential utilization for biomedical applications [8,9].

AgNPs are clusters of zero-valent silver with a size between 1 and 100 nm, and an amount of surface atoms higher than in the bulk material, whereby the scientific community and numerous technologies take advantage of the unique physical, chemical, optical, and biological properties of AgNPs for their use in catalysis, sensing, photonics, electronics, and medical and pharmaceutical engineering [14,15]. Currently, advances in the field of nanotechnology have allowed the reproducible synthesis of materials on a nanoscale using more eco-friendly precursors and leave aside the traditional methodologies which often generate toxic and/or flammable by-products that unavoidably trigger the envi-

* Corresponding author.
** Correspondence to: A. Hollmann, Laboratorio de Compuestos Bioactivos, Centro de Investigaciones en Biofísica Aplicada y Alimentos (CIBAAL), CONICET, Universidad Nacional de Santiago del Estero, RN 9, Km 1125, 4206 Santiago del Estero, Argentina.
Email addresses: p-dalmasso@hotmail.com (P.R. Dalmasso); ahollmann@conicet.gov.ar (A. Hollmann)

https://doi.org/10.1016/j.bbamem.2019.03.011
Received 23 October 2018; Received in revised form 20 February 2019; Accepted 15 March 2019
Available online xxx

ronmental and safety issues [16,17]. In this regard, green synthesis protocols of AgNPs (G-AgNPs) provide an advancement over other methods because they are simple, one step, cost-effective, environment friendly, and relatively reproducible; moreover, they often result in more stable nanomaterials [18]. Thus, green synthesis of AgNPs has been reported using a variety of naturally occurring reagents such as microorganisms, fungi, and especially plant extracts [19–22]. Furthermore, during green synthesis, biological molecules present act not only as reducing agents, but also as natural capping agents in replace of chemical ones. In addition, besides G-AgNPs and its chemically synthesized counterparts have shown not much difference between their morphologies, G-AgNPs exhibited much better antibacterial activity [23,24].

The antibacterial effect of silver-containing nanomaterials, such as metallic AgNPs as well as nanoparticles of silver compounds, has been reported by many researchers [25–27]. Although the highly antibacterial effect of AgNPs has been widely described, their mechanism of action and effects on whole cells has not yet been fully elucidated. In fact, the potent antibacterial and broad-spectrum activity of AgNPs against morphologically and metabolically different microorganisms seems to be correlated with a multifaceted mechanism [28]. It was shown that silver-containing nanomaterials can: *i*) disrupt bacterial metabolic processes [29,30], *ii*) interact with DNA [31], *iii*) increase the cytoplasmic membrane permeability [32,33], and *iv*) generate oxidative stress [34]. However, and in order to consider G-AgNPs as a therapeutic option and overcome clinical setbacks, a worldwide work must be done in order to unravel their mechanisms of action, as well as to manufacture them cost-effectively on a large scale. In this context, in a previous work we showed that the interaction of AgNPs with lipid membranes seems to be a critical step for the resulting antibacterial activity of G-AgNPs coated with aromatic/hydrophobic moieties from chicoric and chlorogenic acids, which were obtained *via* a green chemical synthesis using an aqueous leaf extract of chicory (*Cichorium intybus* L.) [24].

Therefore, the aim of this work was to gain information about the mode of action of green nanosilver with chicoric/chlorogenic acid capping, as well as its cellular target, studying the interaction of these novel G-AgNPs with whole bacteria using *Escherichia coli* and *Staphylococcus aureus* as Gram-negative and Gram-positive models, respectively. Surface characterization techniques, namely zeta potential and atomic force microscopy (AFM), were used to *i*) correlate the G-AgNPs-bacteria attachment with the resulting lethal activity, and *ii*) unravel the effects of this nanomaterial on the bacterial envelope, respectively.

2. Material and methods

2.1. Synthesis of G-AgNPs

Green silver nanoparticles were synthesized employing an experimental method similar to the previously reported [20]. Briefly, the aqueous extract was prepared by decoction of leaf pieces (5 g) of chicory in 100 mL of tridistilled water for 5 min. The resultant extract was filtered using a Whatman No. 1 filter paper. For the synthesis of G-AgNPs, 50 mL of 1 mM $AgNO_3$ (Cicarelli, Argentina) were heated up to 80 °C. Once this temperature was reached, and solution, 5 mL of previously obtained chicory leaf extract were added to the solution, with stirring. During the reaction time of 15 min, both temperature and agitation remained constant. The formation of AgNPs was monitored by UV–vis spectroscopy using a Hewlett Packard 8453 diode-array spectrophotometer.

2.2. Bacterial strains and growth conditions

E. coli ATCC 25929 and *S. aureus* ATCC 25923 were used in this work to evaluate the interaction with the green nanoparticles. To carry out all the tests, both strains were grown overnight in tryptic soy broth (TSB, Britania, Buenos Aires, Argentina) at 37 °C. After incubation, an aliquot of each culture was inoculated in fresh medium and incubated again until reaching an optical density (OD) of 1.

2.3. Bacterial viability

The number of viable bacteria after 1 h incubation with different concentrations of G-AgNPs was quantified as colony forming units (CFU). As a control, the viable count was also carried out when the bacteria were incubated during the same time in growth medium without the nanomaterial. Decimal dilutions were prepared from each of the samples (with and without G-AgNPs) and plated on tryptic soy agar (TSA). Plates were incubated at 37 °C for 18 h and colonies counted. Viability was expressed as CFU/mL. The test was carried out in triplicate. In addition, the antimicrobial activity of the chicory extract (with G-AgNPs) was also tested against *E. coli* or *S. aureus* and no antibacterial effect for both strains was observed (see Supplementary data), which was indicative that this effect was due to G-AgNPs.

2.4. Zeta potential

Zeta potential studies were performed at 25 °C on a Horiba SZ-100 nanoparticle analyzer (Horiba, Kyoto, Japan). Cell dilutions were prepared using saline (NaCl 0.89% w/v). Bacterial suspensions were dispensed into disposable zeta potential cells with gold electrodes and allowed to equilibrate for 10 min at 25 °C. Bacterial concentrations were 2×10^9 CFU/mL in order to acquire high enough count rates. For each sample, the zeta potential was determined from the mean of 10 measurements (500 runs each). The complete experiment was carried out in triplicate for each sample, using independently grown cultures.

2.5. AFM imaging

Particle size analysis and morphological characterization of G-AgNPs were done using a JPK NanoWizard IV atomic force microscope (Berlin, Germany), mounted on a Zeiss Axiovert 200 inverted microscope (Jena, Germany). Images were performed in intermittent contact mode in air, using ACT silicon cantilevers (AppNano, Huntingdon, UK) with a nominal tip radius of 6 nm, typical frequencies of 300 kHz, and a spring constant of 40 N/m. All images were obtained with similar AFM settings (set point, scan rate and gain). Height and error signals were collected and images were analyzed with the JPK image processing software v. 6.0.55. For bacterial surface characterization, the bacterial strains were treated according to previous protocols [35–37]. Briefly, cell suspensions with 1×10^9 CFU/mL were spun down at 3000 × *g* for 10 min and washed twice with 0.85% NaCl to remove the media. A 100 μL droplet of each sample was applied onto a glass slide and allowed to rest at 25 °C for 1 h. After deposition, the sample was rinsed 10 times with Milli-Q water and air-dried at 25 °C. On average, five individual bacterial cells were imaged at high resolution for each sample.

2.6. Surface roughness

The data generated from the AFM height images were used to calculate the surface quadratic roughness of the bacterial cell surface. Using the Gwyddion software v. 2.19 (Czech Metrology Institute, Brno, Czech Republic), the bacterial cell shape was estimated through the application of a mean filter to the raw data. Subtraction of the treated image from the original height image generated a flattened representation of the bacterial cell surface. The surface roughness of a selected area of this flattened image was then calculated from the height standard deviation, *i.e.*, the root-mean-square value (R_{rms}) of the height distribution, using the following equation:

$$R_{rms} = \sqrt{\sum_{i=1}^{n} \frac{(z_i - z_m)^2}{N - 1}} \quad (1)$$

where N is the total number of data points, z_i is the height of the *i*-th point, and z_m is the mean height [38]. Roughness values were measured over the entire bacterial cell surface, on areas with a constant size of $75 \times 75\,nm^2$.

2.7. Membrane leakage

Large unilamellar vesicles (LUVs) with approximately 100 nm of diameter were obtained by extrusion of multilamellar vesicles, as described elsewhere [39]. 1-Palmitoyl-2-oleoyl-*sn*-glycero-3-phosphocholine (POPC) and 1-palmitoyl-2-oleoyl-*sn*-glycero-3-phospho-(1′-*sn*-glycerol) (POPG) were obtained from Avanti Polar Lipids (Alabaster, AL, USA). Phosphate buffer saline (PBS; 20 mM sodium phosphate, 150 mM NaCl) pH 7.4 was used for all measurements. G-AgNPs-induced lipid vesicle leakage was measured by fluorescence spectroscopy, as described previously, using a Varian Cary Eclipse fluorescence spectrophotometer (Mulgrave, Australia) [40–42]. In this assay, the release of 5(6)-carboxyfluorescein (*CF*; Sigma, St. Louis, MO, USA) entrapped into LUVs was monitored. LUVs with encapsulated *CF* were prepared by hydrating the dried lipid film with PBS containing 100 mM *CF* (pH was adjusted to 7.4 with NaOH). Non-encapsulated *CF* was removed by passing the suspension through an EconoPac 10 DG column (Bio-Rad, Richmond, CA, USA) [40]. Aliquots of the liposomal stock preparations (diluted to 10 μM) were incubated with G-AgNPs at 25 °C. Fluorescence was recorded continuously for 30 min, with excitation at 492 nm and emission at 517 nm (5 and 10 nm excitation and emission slits, respectively). The rate of entrapped and released *CF* was estimated by measuring the differences in the fluorescence emission at 517 nm, which increases upon *CF*-leakage from the vesicles. The data for 100% of leakage (*i.e.* complete release of entrapped *CF*) was obtained at the end of the experiment by the Triton X-100 addition to achieve a final concentration of 1% [40–42].

2.8. Statistical analysis

Measurements were done in duplicate from three independent cultures of each group studied. Analysis of variance (ANOVA) followed by Dunnett post-test for multiple comparisons and Student's *t*-test were carried out using the statistical software Graph Pad Prism. Data are shown as the mean value.

3. Results and discussion

Bio-reduction of Ag^+ ions to colloidal nanoparticles was observed by color change from colourless ($AgNO_3$ solution) to yellowish brown (G-AgNPs) and confirmed by AFM. According to the previous results of AgNPs biosynthesized from an aqueous leaf extract of Belgian endive, a variety of *Cichorium intybus* L. [20], the bioactive molecules present in the chicory extract used in this work, mainly chicoric and chlorogenic acids [43], are expected to bind with metal surface, facilitate the formation of a coat over the nanoparticles, and favour in stabilizing the G-AgNPs against agglomeration. Thus, these phenolic compounds play a dual role in the green synthesis of nanosilver acting both as reducing and capping agents and allowing the formation of relatively homogenous spherical nanoparticles with an average diameter around 50 nm, as shown in Fig. 1, and a zeta potential of around −24 mV. These results are in a very good agreement with a previous characterization of these G-AgNPs *via* transmission electron microscopy, dynamic light scattering, and zeta potential, which were also spherical with an average hydrodynamic diameter of 46 nm and a polydispersion index of 0.39 indicating a moderate distribution in the particles size, and had a zeta potential between −27 and −17 mV [24].

In a recent work [24], a biophysical analysis allowed us to probe that green negatively charged-AgNPs can interact with model lipid membranes and bind to a real bacterial membrane using whole *E. coli* bacteria as a model. In this sense, and in order to get an inside in the interaction with whole bacteria and its effects on cell viability, we studied the surface alterations by zeta potential and cell viability by CFU/mL in *E. coli* and *S. aureus* induced by G-AgNPs incubation. As it can be observed in Fig. 2, zeta potential of both tested bacteria become more negative after being incubated with increasing concentrations of G-AgNPs, which is expected due to the negative zeta potential value of this nanomaterial. Beside both bacterial strains showed an increase in the negative value of zeta potential, this effect becomes more noticeable in *E. coli* (with a drop of zeta potential from (−30.1 ± 0.1) mV for untreated cells to (−34.3 ± 0.8) mV with the highest concentration of G-AgNPs tested) than *S. aureus* (with a shift from (−19.0 ± 0.1) mV to (−21.0 ± 0.7) mV). Thus, and in a good correlation with zeta potential shift, a diminution of >1.6 log units was obtained in *E. coli* with the higher concentration of nanomaterial tested (50 pM). On the other hand, only a drop of 0.3 log units was achieved for *S. aureus* at the same concentration of G-AgNPs. These results allow confirming a strong correlation of zeta potential variation with bacterial damage, which is in a good agreement with those previously reported where the zeta potential changes associated with damage in the structures of surface macromolecules and the physiological state of cells [35,36,44].

These results also reinforce the idea that the interaction of these G-AgNPs with bacterial envelops seem be a critical step in the antibacterial activity, as was previously reported [24]. This correlation between membrane interaction and antibacterial activity could explained either because the membrane is one the main target or by allowing the accumulation of G-AgNPs, in that way increasing the local concentration of silver that could lead to the bactericidal activity.

In order to evaluate the direct effect of G-AgNPs on the bacterial envelope, AFM was used as a tool to assess cell damage. AFM orthogonal projections and error images are presented in Fig. 3. After 1 h of incubation with G-AgNPs, several damages were observed in *E. coli*, together with an increase in surface roughness and, in some cases, membrane disruption and leakage of intracellular content (Fig. 3.2). Even though previous transmission electron microscopy studies using chemical AgNPs showed a similar envelope damage [45], it is important to point out that a concentration 1000-fold lower was needed in the present study to obtain comparable results.

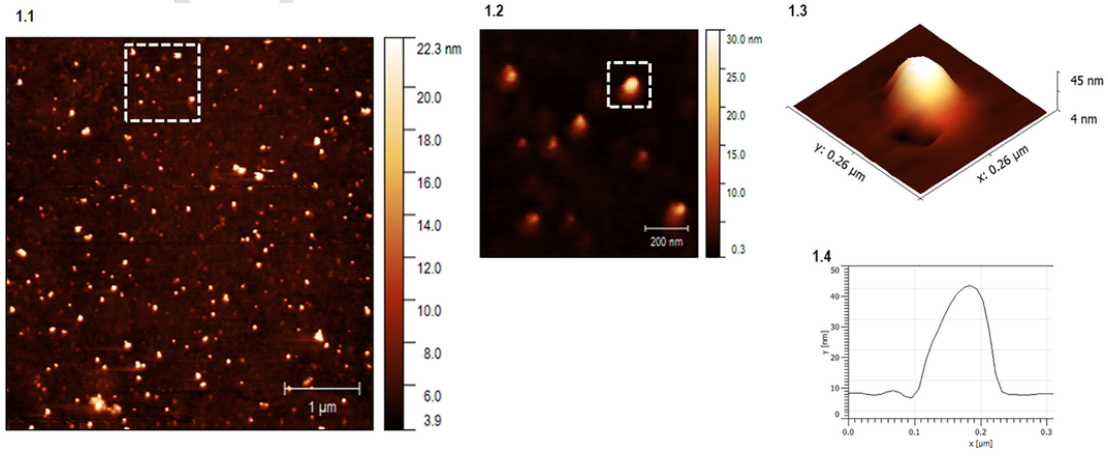

Fig. 1. AFM characterization of G-AgNPs used in this work. 1.1), 1.2), and 1.3) AFM height images of G-AgNPs at a different scale. 1.4) Histogram obtained from height image 1.3).

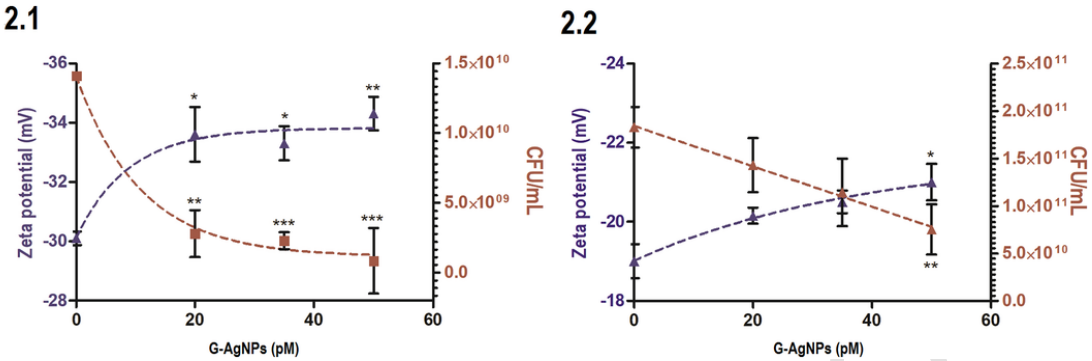

Fig. 2. Zeta potential values and CFU/mL of *E. coli* (2.1) or *S. aureus* (2.2) incubated with different concentrations of G-AgNPs in TSB media. Data represent the averages of three independent measurements. Error bars indicate standard deviations of the mean values. ***$p < .001$; **$p < .01$; *$p < .05$. 1-way ANOVA followed by Dunnett post-test for multiple comparisons *versus* control column (*E. coli* or *S. aureus* without G-AgNPs). Data obtained were fitted with a one-phase exponential decay model using the GraphPad Prism software.

As previously indicated, the aromatic/hydrophobic moieties from the main phenolic compounds in chicory extract adsorbed on G-AgNPs seem to promote the interactions with the hydrocarbon chain of lipids, favouring a close contact of this nanomaterial with the lipid surface [24,46,47], which could explain the strong antibacterial activity of green AgNPs with respect to the chemically-obtained ones [24]. Some structural alterations on *S. aureus* can be observed in Fig. 3.4; however, the changes on the cell surface were much less noticeable than for *E. coli*, in good agreement with the zeta potential data showed in Fig. 2.2. This divergence could be due to the structural and composition differences between the cell wall and membranes of Gram-positive and Gram-negative bacteria, namely at the level of the thickness of the peptidoglycan layer (*S. aureus*) and the presence of an outer membrane containing lipopolysaccharides (*E. coli*) [48].

Additionally, a quantitative characterization of the damage exerted by G-AgNPs incubation was carried out calculating the roughness of the cell surface of both control and treated bacteria (Fig. 4). The surface roughness of untreated *E. coli* cells was (1.04 ± 0.01) nm and (0.7 ± 0.2) nm for *S. aureus* cells, which is in good agreement with previously published data [38]. As it can be seen in Fig. 4, the surface roughness values were significantly affected in both bacterial strains studied exposed to green nanosilver. However, the changes were more noticeable in *E. coli* ((2.7 ± 1) nm) than *S. aureus* ((1.6 ± 0.7) nm) cells, in good agreement with the zeta potential and AFM data shown above. It is important to remark that future studies on the effect of these green nanoparticles on other Gram-positive and Gram-negative bacteria are necessary to evaluate their potential application as a new antibacterial agent.

Overall, the results obtained demonstrate that G-AgNPs were able to attach and disrupt the bacterial envelope, with a more noticeable effect on *E. coli* cells. One possible explanation for these findings is that lipid membranes could be one of the targets of nanosilver, as reported by other authors [28,49]. The fact that Gram-negative bacteria exhibit an outer membrane may explain the major damage in comparison with the Gram-positive *S. aureus* cells. Then, and in order to test this hypothesis for the mode of action of these novel G-AgNPs, leakage experiments were conducted in model lipid membranes (*i.e.*, liposomes) employing LUVs composed of POPC:POPG (5:1) as a model for the bacterial membrane [50,51]. Interestingly, as shown in Fig. 5, no release of liposomally entrapped *CF* was observed, indicating that the G-AgNPs in a concentration similar to the tested in the AFM experiments were not able to induce disruption effects on the model membrane system. Only after the addition of 1% Triton X-100, *CF* entrapped was able to leak from the liposomes in the external media.

The fact that a massive damage, especially in *E. coli*, was observed by AFM in the cell envelope, including intracellular content leakage, but no leakage was observed in the model membranes used, suggests that in the mode of action of G-AgNPs should involve other phenomena that lead to envelope damage. Although the interfacial interaction of this nanomaterial with model lipid membranes causes no disturbance *per se* of lipid packing, still remains as essential step for the G-AgNPs accumulation on the cell envelope, acting as a local silver reservoir or as a Trojan horse that *via* an oxidative dissolution proccess can release a high enough concentration of toxic Ag^+ ions into or close to the bacterial cell [5]. Thus, the Ag^+ ions released may: i) interact with thiol-containing proteins in the cell wall, affecting their biological functions and cell permeability; ii) penetrate the cell wall and enter into the cells, subsequently turning DNA into a condensed form; and, iii) generate reactive oxygen species [5,52]. All these phenomena can lead to cell envelope damage or even cell death. In this sense, a study using *E. coli* confirmed that AgNPs accumulation on the cell membrane creates gaps in the integrity of the bilayer, leading to a permeability increase and finally bacterial cell death [49]. In this scenario, it is important to highlight that recent research has shown that the release of Ag^+ ions from functionalized silver nanostructures can be controlled more efficiently and ideally released fast enough to kill bacteria but slowly enough to overcome the toxicity issue, mainly to the mammalian cells [9,16].

4. Conclusions

The findings of the present study lead to the conclusion that the potent antibacterial and broad-spectrum activity of G-AgNPs against morphologically and metabolically different microorganism correlates with a multifaceted mechanism by which this nanomaterial induces bacterial cell distortion and death. To the best of our knowledge, this is the first study that gives direct evidences that G-AgNPs are able to induce several damages on the bacterial envelope. This was achieved using surface characterization techniques (zeta potential and AFM) and leakage measurements. G-AgNPs accumulation on the bacterial membrane *via* the primary AgNPs-lipid membrane interaction, without lipid packing disruption, seem to be an essential step to the desired biological effect. G-AgNPs immobilized on the bacterial surface may be able to produce a Trojan horse effect, locally releasing high concentration of antibacterial silver ions. Subsequently, the interaction of silver ions with macromolecule targets may cause alterations of cell morphology, interfere with the DNA replication process, induce oxidative stress and, consequently, lead to bacterial death. Therefore, the green synthesis technology represents a promising approach for cost-effective and environmental-friendly production of nanosilver, with enhanced antibacterial properties.

Supplementary data to this article can be found online at https://doi.org/10.1016/j.bbamem.2019.03.011.

Transparency document

The Transparency document associated with this article can be found, in online version.

Acknowledgments and funding

Authors acknowledge the financial support of CONICET (PIP 11220130100702CO, PIP 11220130100383CO), CONICET-UNSE (PIO

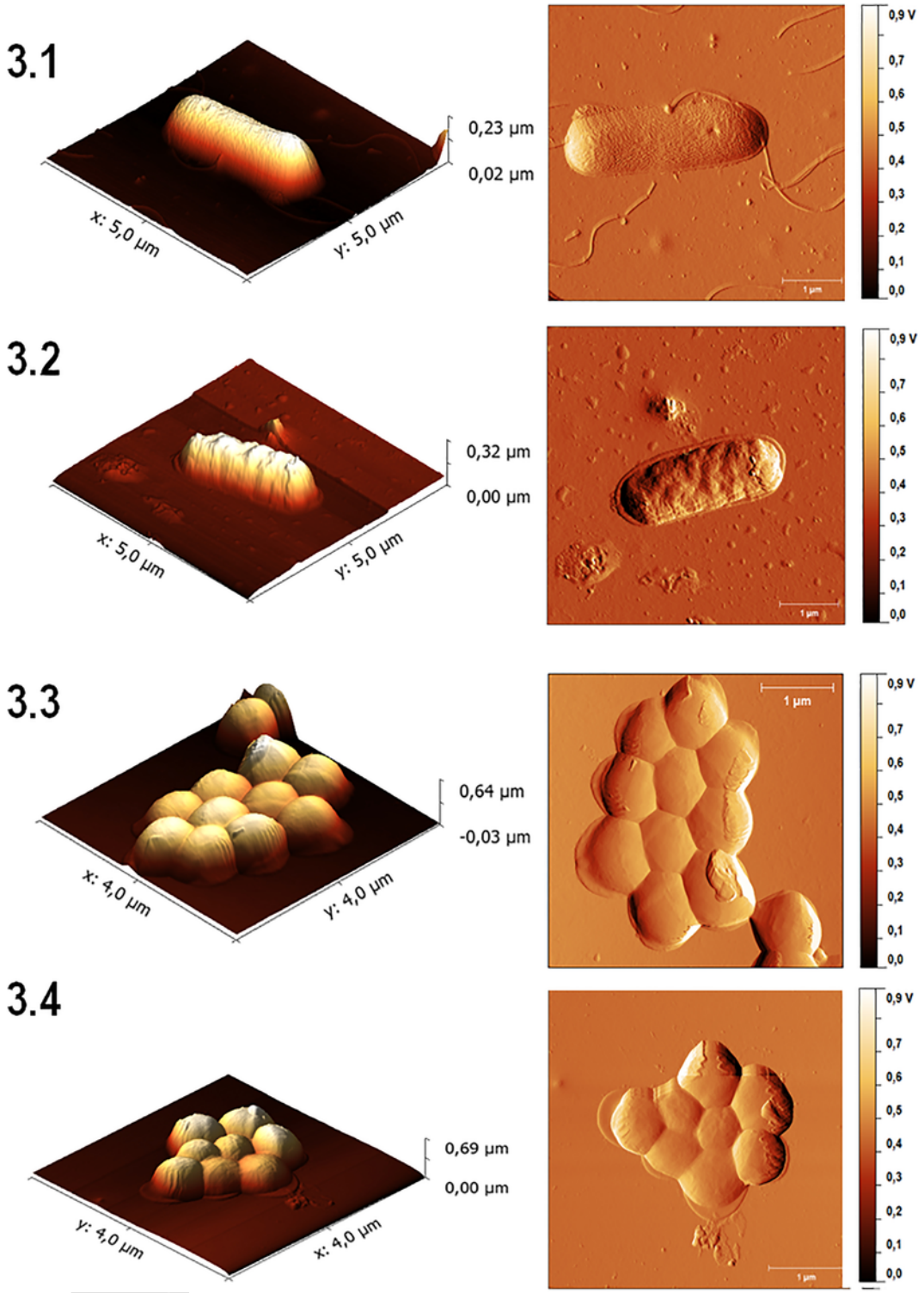

Fig. 3. AFM orthogonal projections (left) and AFM error images (right) of (3.1) *E. coli* in the absence of nanoparticles, (3.2) *E. coli* incubated 1 h with 5 pM G-AgNPs, (3.3) *S. aureus* in the absence of nanoparticles, and (3.4) *S. aureus* incubated 1 h with 5 pM G-AgNPs.

14520140100013CO) and ANPCyT-FONCyT (PICT 2017-2349, PICT 2014-1663), from Argentina, and Fundação para a Ciência e a Tecnologia – Ministério da Ciência, Tecnologia e Ensino Superior (FCT-MCTES), from Portugal. PRD, BALM and AH are members of the Research Career of CONICET. APVMF acknowledges a fellowship from CONICET.

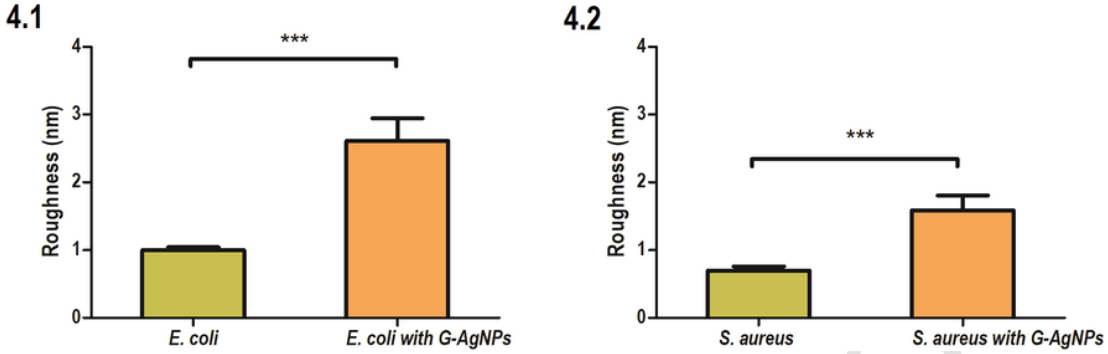

Fig. 4. Surface roughness (calculated based on the AFM images) of *E. coli* and *S. aureus* incubated 1 h without and with 5 pM G-AgNPs. Data represent mean ± standard deviation. ***$p < .001$, unpaired Student's *t*-test.

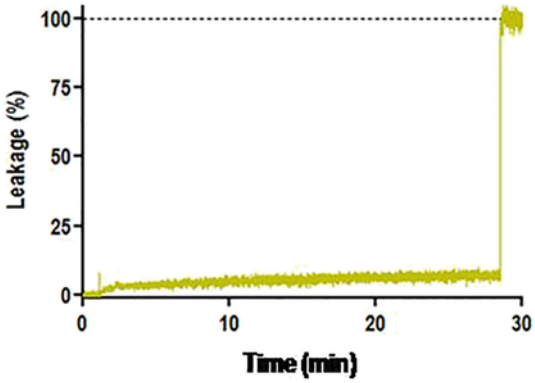

Fig. 5. Leakage of liposomes of POPC:POPG (5:1) in the presence of G-AgNPs. Liposome suspension contained 0.1 mM total phospholipid concentration and 5 pM of G-AgNPs, as a function of time. Triton X-100 was added at 27 min, in order to achieve 100% of leakage.

References

[1] R.Y. Pelgrift, A.J. Friedman, Nanotechnology as a therapeutic tool to combat microbial resistance, Adv. Drug Deliv. Rev. 65 (2013) 1803–1815, https://doi.org/10.1016/j.addr.2013.07.011.

[2] C. Furusawa, T. Horinouchi, T. Maeda, Toward prediction and control of antibiotic-resistance evolution, Curr. Opin. Biotechnol. 54 (2018) 45–49, https://doi.org/10.1016/j.copbio.2018.01.026.

[3] A.J. Huh, Y.J. Kwon, "Nanoantibiotics": a new paradigm for treating infectious diseases using nanomaterials in the antibiotics resistant era, J. Control. Release 156 (2011) 128–145, https://doi.org/10.1016/j.jconrel.2011.07.002.

[4] M.K. Rai, S.D. Deshmukh, A.P. Ingle, A.K. Gade, Silver nanoparticles: the powerful nanoweapon against multidrug-resistant bacteria, J. Appl. Microbiol. 112 (2012) 841–852, https://doi.org/10.1111/j.1365-2672.2012.05253.x.

[5] B. Le Ouay, F. Stellacci, Antibacterial activity of silver nanoparticles: a surface science insight, Nano Today 10 (2015) 339–354, https://doi.org/10.1016/j.nantod.2015.04.002.

[6] A.F. Halbus, T.S. Horozov, V.N. Paunov, Colloid particle formulations for antimicrobial applications, Adv. Colloid Interf. Sci. 249 (2017) 134–148, https://doi.org/10.1016/j.cis.2017.05.012.

[7] A. Mandal, V. Meda, W.J. Zhang, K.M. Farhan, A. Gnanamani, Synthesis, characterization and comparison of antimicrobial activity of PEG/TritonX-100 capped silver nanoparticles on collagen scaffold, Colloids Surf. B: Biointerfaces 90 (2012) 191–196, https://doi.org/10.1016/j.colsurfb.2011.10.021.

[8] A. Mandal, S. Sekar, K.M. Seeni Meera, A. Mukherjee, T.P. Sastry, A.B. Mandal, Fabrication of collagen scaffolds impregnated with sago starch capped silver nanoparticles suitable for biomedical applications and their physicochemical studies, Phys. Chem. Chem. Phys. 16 (2014) 20175–20183, https://doi.org/10.1039/c4cp02554g.

[9] A. Mandal, S. Sekar, N. Chandrasekaran, A. Mukherjee, T.P. Sastry, Synthesis, characterization and evaluation of collagen scaffolds crosslinked with aminosilane functionalized silver nanoparticles: in vitro and in vivo studies, J. Mater. Chem. B 3 (2015) 3032–3043, https://doi.org/10.1039/C4TB02124J.

[10] A. Mandal, S. Sekar, N. Chandrasekaran, A. Mukherjee, T. Sastry, Poly(ethylene) glycol–capped silver and magnetic nanoparticles: synthesis, characterization, and comparison of bactericidal and cytotoxic effects, Proc. Inst. Mech. Eng. H 227 (2013) 1224–1236, https://doi.org/10.1177/0954411913499290.

[11] R. Prucek, J. Tuček, M. Kilianová, A. Panáček, L. Kvítek, J. Filip, M. Kolář, K. Tománková, R. Zbořil, The targeted antibacterial and antifungal properties of magnetic nanocomposite of iron oxide and silver nanoparticles, Biomaterials 32 (2011) 4704–4713, https://doi.org/10.1016/j.biomaterials.2011.03.039.

[12] K.-S. Huang, D.-B. Shieh, C.-S. Yeh, P.-C. Wu, F.-Y. Cheng, Antimicrobial applications of water-dispersible magnetic nanoparticles in biomedicine, Curr. Med. Chem. 21 (2014) 3312–3322, https://doi.org/10.2174/09298673216614030410175 2.

[13] G.R. Rodrigues, C. López-Abarrategui, I. de la Serna Gómez, S.C. Dias, A.J. Otero-González, O.L. Franco, Antimicrobial magnetic nanoparticles based-therapies for controlling infectious diseases, Int. J. Pharm. 555 (2019) 356–367, https://doi.org/10.1016/j.ijpharm.2018.11.043.

[14] Q.H. Tran, V.Q. Nguyen, A.-T. Le, Silver nanoparticles: synthesis, properties, toxicology, applications and perspectives, Adv. Nat. Sci. Nanosci. Nanotechnol. 4 (2013)033001https://doi.org/10.1088/2043-6262/4/3/033001.

[15] X. Chen, H.J. Schluesener, Nanosilver: a nanoproduct in medical application, Toxicol. Lett. 176 (2008) 1–12, https://doi.org/10.1016/j.toxlet.2007.10.004.

[16] S.K. Das, M.M.R. Khan, T. Parandhaman, F. Laffir, A.K. Guha, G. Sekaran, A.B. Mandal, Nano-silica fabricated with silver nanoparticles: antifouling adsorbent for efficient dye removal, effective water disinfection and biofouling control, Nanoscale 5 (2013) 5549–5560, https://doi.org/10.1039/c3nr00856h.

[17] H. Duan, D. Wang, Y. Li, Green chemistry for nanoparticle synthesis, Chem. Soc. Rev. 44 (2015) 5778–5792, https://doi.org/10.1039/c4cs00363b.

[18] J. Mittal, A. Batra, A. Singh, M.M. Sharma, Phytofabrication of nanoparticles through plant as nanofactories, Adv. Nat. Sci. Nanosci. Nanotechnol. 5 (2014)043002https://doi.org/10.1088/2043-6262/5/4/043002.

[19] O.V. Kharissova, H.V.R. Dias, B.I. Kharisov, B.O. Pérez, V.M.J. Pérez, The greener synthesis of nanoparticles, Trends Biotechnol. 31 (2013) 240–248, https://doi.org/10.1016/j.tibtech.2013.01.003.

[20] M.N. Gallucci, J.C. Fraire, A.P.V. Ferreyra Maillard, P.L. Páez, I.M. Aiassa Martínez, E.V. Pannunzio Miner, E.A. Coronado, P.R. Dalmasso, Silver nanoparticles from leafy green extract of Belgian endive (Cichorium intybus L. var. sativus): biosynthesis, characterization, and antibacterial activity, Mater. Lett. 197 (2017) 98–101, https://doi.org/10.1016/j.matlet.2017.03.141.

[21] M.A. Quinteros, I.M. Aiassa Martínez, P.R. Dalmasso, P.L. Páez, Silver nanoparticles: biosynthesis using an ATCC reference strain of Pseudomonas aeruginosa and activity as broad spectrum clinical antibacterial agents, Int. J. Biomater. 2016 (2016) 1–7, https://doi.org/10.1155/2016/5971047.

[22] M.S. Dzul-Erosa, M.M. Cauich-Díaz, T.A. Razo-Lazcano, M. Avila-Rodriguez, J.A. Reyes-Aguilera, M.P. González-Muñoz, Aqueous leaf extracts of Cnidoscolus chayamansa (Mayan chaya) cultivated in Yucatán México. Part II: uses for the phytomediated synthesis of silver nanoparticles, Mater. Sci. Eng. C 91 (2018) 838–852, https://doi.org/10.1016/j.msec.2018.06.007.

[23] U.K. Parashar, V. Kumar, T. Bera, P.S. Saxena, G. Nath, S.K. Srivastava, R. Giri, A. Srivastava, Study of mechanism of enhanced antibacterial activity by green synthesis of silver nanoparticles, Nanotechnology 22 (2011)415104https://doi.org/10.1088/0957-4484/22/41/415104.

[24] A.P.V. Ferreyra Maillard, P.R. Dalmasso, B.A. López de Mishima, A. Hollmann, Interaction of green silver nanoparticles with model membranes: possible role in the antibacterial activity, Colloids Surf. B: Biointerfaces 171 (2018) 320–326, https://doi.org/10.1016/j.colsurfb.2018.07.044.

[25] M. Rai, A. Yadav, A. Gade, Silver nanoparticles as a new generation of antimicrobials, Biotechnol. Adv. 27 (2009) 76–83, https://doi.org/10.1016/j.biotechadv.2008.09.002.

[26] C. Marambio-Jones, E.M.V. Hoek, A review of the antibacterial effects of silver nanomaterials and potential implications for human health and the environment, J. Nanopart. Res. 12 (2010) 1531–1551, https://doi.org/10.1007/s11051-010-9900-y.

[27] S. Eckhardt, P.S. Brunetto, J. Gagnon, M. Priebe, B. Giese, K.M. Fromm, Nanobio silver: its interactions with peptides and bacteria, and its uses in medicine, Chem. Rev. 113 (2013) 4708–4754, https://doi.org/10.1021/cr300288v.

[28] G. Franci, A. Falanga, S. Galdiero, L. Palomba, M. Rai, G. Morelli, M. Galdiero, Silver nanoparticles as potential antibacterial agents, Molecules 20 (2015) 8856–8874, https://doi.org/10.3390/molecules20058856.

[29] L. Cui, P. Chen, S. Chen, Z. Yuan, C. Yu, B. Ren, K. Zhang, In situ study of the antibacterial activity and mechanism of action of silver nanoparticles by surface-enhanced raman spectroscopy, Anal. Chem. 85 (2013) 5436–5443, https://doi.org/10.1021/ac400245j.

[30] H.H. Lara, N.V. Ayala-Núñez, L. del C. Ixtepan Turrent, C. Rodríguez Padilla, Bactericidal effect of silver nanoparticles against multidrug-resistant bacteria, World J. Microbiol. Biotechnol. 26 (2010) 615–621, https://doi.org/10.1007/s11274-009-0211-3.

[31] W.-R. Li, X.-B. Xie, Q.-S. Shi, S.-S. Duan, Y.-S. Ouyang, Y.-B. Chen, Antibacterial effect of silver nanoparticles on Staphylococcus aureus, BioMetals 24 (2011) 135–141, https://doi.org/10.1007/s10534-010-9381-6.

[33] J.R. Morones, J.L. Elechiguerra, A. Camacho, K. Holt, J.B. Kouri, J.T. Ramírez, M.J. Yacaman, The bactericidal effect of silver nanoparticles, Nanotechnology 16 (2005) 2346–2353, https://doi.org/10.1088/0957-4484/16/10/059.

[34] M.A. Quinteros, V. Cano Aristizábal, P.R. Dalmasso, M.G. Paraje, P.L. Páez, Oxidative stress generation of silver nanoparticles in three bacterial genera and its relationship with the antimicrobial activity, Toxicol. in Vitro 36 (2016) 216–223, https://doi.org/10.1016/j.tiv.2016.08.007.

[35] M.M. Domingues, P.M. Silva, H.G. Franquelim, F.A. Carvalho, M.A.R.B. Castanho, N.C. Santos, Antimicrobial protein rBPI21-induced surface changes on Gram-negative and Gram-positive bacteria, Nanomedicine 10 (2014) 543–551, https://doi.org/10.1016/j.nano.2013.11.002.

[36] B.M. Bravo-Ferrada, S. Gonçalves, L. Semorile, N.C. Santos, N.S. Brizuela, E. Elizabeth Tymczyszyn, A. Hollmann, Cell surface damage and morphological changes in Oenococcus oeni after freeze-drying and incubation in synthetic wine, Cryobiology 82 (2018) 15–21, https://doi.org/10.1016/j.cryobiol.2018.04.014.

[37] M.M. Domingues, M.R. Felício, S. Gonçalves, Antimicrobial Peptides: Effect on Bacterial Cells, in: Humana Press, NY, New York, 2019233–242, https://doi.org/10.1007/978-1-4939-8894-5_13.

[38] C.S. Alves, M.N. Melo, H.G. Franquelim, R. Ferre, M. Planas, L. Feliu, E. Bardají, W. Kowalczyk, D. Andreu, N.C. Santos, M.X. Fernandes, M.A.R.B. Castanho, Escherichia coli cell surface perturbation and disruption induced by antimicrobial peptides BP100 and pepR, J. Biol. Chem. 285 (2010) 27536–27544, https://doi.org/10.1074/jbc.M110.130955.

[39] L.D. Mayer, M.J. Hope, P.R. Cullis, Vesicles of variable sizes produced by a rapid extrusion procedure, Biochim. Biophys. Acta Biomembr. 858 (1986) 161–168, https://doi.org/10.1016/0005-2736(86)90302-0.

[40] J. Turánek, A. Kašná, D. Záluská, J. Neča, Preparation of sterile liposomes by proliposome-liposome method, Methods Enzymol. 367 (2003) 111–125, https://doi.org/10.1016/S0076-6879(03)67009-6.

[41] M.M. Domingues, M.A.R.B. Castanho, N.C. Santos, rBPI21 promotes lipopolysaccharide aggregation and exerts its antimicrobial effects by (hemi)fusion of PG-containing membranes, PLoS One 4 (2009)e8385https://doi.org/10.1371/journal.pone.0008385.

[42] A. Marín-Menéndez, C. Montis, T. Díaz-Calvo, D. Carta, K. Hatzixanthis, C.J. Morris, M. McArthur, D. Berti, Antimicrobial nanoplexes meet model bacterial membranes: the key role of cardiolipin, Sci. Rep. 7 (2017)41242https://doi.org/10.1038/srep41242.

[43] M. Innocenti, S. Gallori, C. Giaccherini, F. Ieri, F.F. Vincieri, N. Mulinacci, Evaluation of the phenolic content in the aerial parts of different varieties of Cichorium intybus L, J. Agric. Food Chem. 53 (2005) 6497–6502, https://doi.org/10.1021/jf050541d.

[44] B.M. Bravo-Ferrada, N. Brizuela, E. Gerbino, A. Gómez-Zavaglia, L. Semorile, E.E. Tymczyszyn, Effect of protective agents and previous acclimation on ethanol resistance of frozen and freeze-dried Lactobacillus plantarum strains, Cryobiology 71 (2015) 522–528, https://doi.org/10.1016/j.cryobiol.2015.10.154.

[45] W.R. Li, X.B. Xie, Q.S. Shi, H.Y. Zeng, Y.S. Ou-Yang, Y. Ben Chen, Antibacterial activity and mechanism of silver nanoparticles on Escherichia coli, Appl. Microbiol. Biotechnol. 85 (2010) 1115–1122, https://doi.org/10.1007/s00253-009-2159-5.

[46] J. Gao, O. Zhang, J. Ren, C. Wu, Y. Zhao, Aromaticity/bulkiness of surface ligands to promote the interaction of anionic amphiphilic gold nanoparticles with lipid bilayers, Langmuir 32 (2016) 1601–1610, https://doi.org/10.1021/acs.langmuir.6b00035.

[47] J.V. Maya Girón, R.V. Vico, B. Maggio, E. Zelaya, A. Rubert, G. Benítez, P. Carro, R.C. Salvarezza, M.E. Vela, Role of the capping agent in the interaction of hydrophilic Ag nanoparticles with DMPC as a model biomembrane, Environ. Sci. Nano 3 (2016) 462–472, https://doi.org/10.1039/c6en00016a.

[48] T.J. Silhavy, D. Kahne, S. Walker, The bacterial cell envelope, Cold Spring Harb. Perspect. Biol. 2 (2010) a000414, https://doi.org/10.1101/cshperspect.a000414.

[49] M. Rai, K. Kon, A. Ingle, N. Duran, S. Galdiero, M. Galdiero, Broad-spectrum bioactivities of silver nanoparticles: the emerging trends and future prospects, Appl. Microbiol. Biotechnol. 98 (2014) 1951–1961, https://doi.org/10.1007/s00253-013-5473-x.

[50] P. Maturana, M. Martinez, M.E. Noguera, N.C. Santos, E.A. Disalvo, L. Semorile, P.C. Maffia, A. Hollmann, Lipid selectivity in novel antimicrobial peptides: implication on antimicrobial and hemolytic activity, Colloids Surf. B: Biointerfaces 153 (2017) 152–159, https://doi.org/10.1016/j.colsurfb.2017.02.003.

[51] A. Hollmann, M. Martínez, M.E. Noguera, M.T. Augusto, A. Disalvo, N.C. Santos, L. Semorile, P.C. Maffía, Role of amphipathicity and hydrophobicity in the balance between hemolysis and peptide-membrane interactions of three related antimicrobial peptides, Colloids Surf. B: Biointerfaces 141 (2016) 528–536, https://doi.org/10.1016/j.colsurfb.2016.02.003.

[52] Q.L. Feng, J. Wu, G.Q. Chen, F.Z. Cui, T.N. Kim, J.O. Kim, A mechanistic study of the antibacterial effect of silver ions on *Escherichia coli* and *Staphylococcus aureus*, J. Biomed. Mater. Res. 52 (2000) 662–668.doi:10.1002/1097-4636(20001215)52:4<662::AID-JBM10>3.0.CO;2-3.

The number of viable bacteria after 1 h incubation with different concentrations of G-AgNPs was quantified as colony forming units (CFU). As a control, the viable count was also carried out when the bacteria were incubated during the same time in growth medium without the nanomaterial. Decimal dilutions were prepared from each of the samples (with and without G-AgNPs) and plated on tryptic soy agar (TSA). Plates were incubated at 37 °C for 18 h and colonies counted. Viability was expressed as CFU/mL. The test was carried out in triplicate. In addition, the antimicrobial activity of the chicory extract (with G-AgNPs) was also tested against *E. coli* or *S. aureus* and no antibacterial effect for both strains was observed (see Supplementary data), which was indicative that this effect was due to G-AgNPs.